Monitoring lipid oxidation in multiple emulsions by near infrared spectroscopy

Laetitia Boisset, Pascale de Caro, Ivana Stojmilovic, Sophie Thiebaud-Roux, Cécile Levasseur-Garcia

Received: 27 November 2023 | Revised: 29 February 2024 | Accepted: 5 March 2024

DOI: 10.1002/ejlt.202300267

European Journal of
Lipid Science and Technology

RESEARCH ARTICLE

Monitoring lipid oxidation in multiple emulsions by near infrared spectroscopy

Laetitia Boisset[1] | **Pascale de Caro**[1] | **Ivana Stojmilovic**[1] | **Sophie Thiebaud-Roux**[1] | **Cécile Levasseur-Garcia**[2]

[1]Laboratoire de Chimie Agro-industrielle (LCA), Université de Toulouse, INRAE, Toulouse INP, Toulouse, France

[2]Laboratoire de Chimie Agro-industrielle (LCA), Université de Toulouse, INRAE, Toulouse INP, INP-Purpan, Toulouse, France

Correspondence
Pascale de Caro, Laboratoire de Chimie Agro-industrielle, 4 allée Emile Monso - BP 44362, 31030 TOULOUSE Cedex 4, France.
Email: pascale.decaro@ensiacet.fr

Funding information
National agency for research and technology (ANRT); Colibri; National Research Agency under the Program for Future Investments, Grant/Award Number: ANR-18-EURE-0021

Abstract

Lipid oxidation has an impact on the quality and properties of fat-containing products that are commonly produced by cosmetics or coatings industries. In this study, a water-in-oil-in-water emulsion (48% w/w of pre-polymerized linseed oil stabilized with alkylpolyglucoside) was subjected to oxidation under accelerated aging conditions at 50°C over 15 days. After fat extraction from emulsion, peroxide, and *p*-anisidine values were measured using standardized methods. The application of near infrared spectroscopy (NIRS) in conjunction with chemometrics was investigated to assess the quality parameters of emulsions under accelerated aging within closed flasks. Significant variations were observed across the following spectral regions: 7541–5948, 5739–3657, and 3645–3637 cm^{-1}. Partial least squares regression discriminant analysis, possibly combined with multiplicative scattering correction preprocessing, proved to be a powerful method to classify the emulsions according to two oxidation levels defined by periods A and B. The performances of the prediction model were characterized by a precision of 85%, a predictive value of period A of 98%, a sensitivity of 99%, a specificity of 81%, and an accuracy of 90%. Thus, we demonstrate that NIRS is a suitable analytical method to discriminate emulsions according to their aging behavior. *Practical Applications*: The PLS-DA method coupled to near infrared spectroscopy analyses is adapted to assess the chemical degradations of vegetable oil–based emulsions due to lipid oxidation. This tool is interesting for *at-line* or *off-line* monitoring of emulsions during their storage. As it is a fast and nondestructive method, the quality control of a formulation stored in a closed glass container is facilitated. This method could also be used to determine the effectiveness of an antioxidant or a drier in emulsions, respectively, prepared for cosmetics and coatings.

Abbreviations: AV, anisidine value; D1, first derivative transformations of Savitzky–Golay; D2, second derivative transformations of Savitzky–Golay; D3, third transformations of Savitzky–Golay; FN, false negative rate; FP, false positive rate; MSC, multiplicative scattering correction; NIR, near infrared; NIRS, near infrared spectroscopy; O/W, oil-in-water; O/W/O, oil-in-water-in-oil; PLS-DA, partial least square regression with discriminant analysis; PV, peroxide value; SNV, standard normal variate; TN, true negative rate; TP, true positive rate; TV, total oxidation value; W/O, water-in-oil; W/O/W, water-in-oil-in-water.

KEYWORDS
aging, emulsion, lipid oxidation, near infrared spectroscopy, PLS-DA

1 | INTRODUCTION

Vegetable oil–based emulsions are dispersed systems stabilized by surfactants or emulsifiers. Depending on how they are emulsified, these biphasic or triphasic media could be of different types, such as oil-in-water (O/W), water-in-oil (W/O), oil-in-water-in-oil (O/W/O), or water-in-oil-in-water (W/O/W).[1] Such emulsions find utility in various formulations used in the development of bio-lubricants, environmentally friendly coatings, pharmaceuticals, food products, and more.[1] Emulsions serve to limit lipid content in the formulation, create thin protective surface films, or to vectorize active molecules. Hence, it is important to maintain the quality of an emulsion over time to avoid altering the properties of formulated products. The quality of an emulsion depends on its physical, chemical, and biological stability. The chemical degradation of emulsions mainly occurs through the lipid oxidation process, which has usually been studied for oils in the bulk state.[2] In the case of an emulsion, the interaction between the oil and the aqueous phases can potentially influence the oxidation process according to the amount of pro-oxidant compounds (such as metals) present in the aqueous phase.[3,4] Poyato et al. have found that multiple and simple emulsions with added antioxidants have similar oxidative stabilities.[5]

Lipid oxidation leads to the formation of primary and secondary oxidation compounds, some of which are involved in polymerization reactions. Even though these reactions are useful for forming coating films, it is necessary to avoid the formation of these oxidation compounds during storage of the emulsion, which can be between a few weeks and several months. For pharmaceutical applications, the inhibition of lipid oxidation is essential to ensure the safety of the delivery system.[6,7] The oxidative state of oils is conventionally determined by titrating the oxidation products such as peroxides and aldehydes.[8,9] Previous works have reported analyses of these oxidation products by chromatography, Nuclear Magnetic Resonance, or by measuring oxygen consumption.[8,10,11] It is recommended to employ a minimum of two analytical techniques to comprehensively characterize the entire deterioration process.[10] However, these methods require the extraction of oil from the bulk, which makes sample preparation time-consuming while requiring the use of toxic products.[10] To address these issues, analytical methods such as Fourier transform mid-infrared (FTIR) spectroscopy have been developed to study lipid oxidation in emulsions, with the diene or peroxide content serving as a reference to define the extent of oxidation.[12,13] FTIR allows a fast and direct analysis but requires sampling. Near infrared spectroscopy (NIRS) has also been reported as a powerful technique that allows to directly correlate spectral changes with the chemical alteration of lipids.[14,15]

NIRS is an analysis method that uses the near infrared (NIR) region of the electromagnetic spectrum between 780 and 2500 nm, corresponding to overtone and combination bands.[16] This method has already been applied to in situ monitoring of lipid oxidation in O/W emulsions (using a fiber optic probe), and the conjugated diene values have been correlated to the recorded NIR spectra for the first 7 days of aging at 25°C.[9]

The originality of the present study is to develop a noninvasive method using NIRS to assess the oxidative state of a multiple emulsion during its storage. So, a new sampling method was tested to carry out *at-line* or *off-line* analysis of the emulsion through the glass container in which the emulsion was stored. This study is based on kinetically tracking the chemical stability of an emulsion under accelerated aging conditions. The chosen reference methods (peroxide and *p*-anisidine values [AVs]) take into account the different oxidation products of lipids.[7] A chemometric strategy aims to correlate the oxidation state with NIR data.

2 | MATERIALS AND METHODS

A pre-polymerized linseed oil was produced by a plasma activation process under hydrogen flow, according to the device described by Godfroid et al.[17] The resulting oil has the following characteristics: an iodine value of 135.2 g 100 g^{-1}, an acid value of 2.47 mg KOH g^{-1}, a saponification value of 188 mg KOH g^{-1}, and a rate of unsaponifiable matter of 0.61%.

Simulsol SL26C (alkylpolyglucoside), supplied by Seppic, was used as the bio-based surfactant. The materials used for lipid extraction were 2,2,4-trimethylpentane ≥99.5% (CAS number 540-84-1), 2-propanol (CAS number 67-63-0) purchased from VWR Chemicals; sodium chloride (CAS number 7647-14-5) and magnesium sulfate (CAS number 7487-88-9) were purchased from Sigma-Aldrich. For the measurement of peroxides and *p*-AVs, glacial acetic acid (CAS number 64-19-7) was purchased from Panreac, potassium iodide (CAS number 7681-11-0) and sodium thiosulfate (CAS number 7772-98-7) were acquired from Sigma-Aldrich, and 4-methoxyaniline ≥98.5% (CAS number 104-94-9) was obtained from Thermo Fisher Scientific.

2.1 | Preparation of emulsions and aliquots

Multiple emulsions (W/O/W) were prepared using the phase inversion technique. The oil phase was prepared by combining 48% (w/w) of pre-polymerized linseed oil with 3% (w/w) of alkylpolyglucoside. Demineralized water was added to the oil phase at the rate of 0.58 mL min^{-1} with the help of a peristaltic pump (Labbox) under continuous stirring (150 rpm) using an emulsification stirrer (Ø42 mm, IKA); sixteen emulsions were prepared. Each emulsion of 90 g was transferred into a 250 mL capped bottle (61.7 mm internal diameter). The samples

were kept at 50°C for 15 days. Eleven of these emulsions were used in reference methods, and the five remaining were analyzed by NIR spectroscopy daily for 15 days. The lipid phase was extracted according to the method of Daoud et al., with slight modifications.[12] A 150 mL volume of the mixture isooctane:2-propanol (3:1) was prepared in a bottle, to which 0.5 g of sodium chloride and 60 g of the emulsion were added and mixed manually for 1 min. After 30 min of decantation, the organic phase was separated and dried with magnesium sulfate before analysis.

2.2 | Peroxide value

The peroxide value (PV) was used as the reference to determine the primary oxidation products.

PVs were measured according to the European standard NF EN ISO 27107:2010 with slight modifications.[18] A 26 mL volume of the previously extracted oil was diluted by adding 50 mL of a mixture of glacial acetic acid and isooctane (3:2). Next, 0.5 mL of a saturated potassium iodide solution was added. After stirring for 1 min, 150 mL of water was added. The sample was potentiometrically titrated by end point determination using 0.01 N sodium thiosulfate solution. Three aliquots were analyzed for each emulsion. In parallel, a blank test (without oil) was also performed. PVs were expressed in milliequivalents of active oxygen per kilogram.

2.3 | Anisidine value

The *p*-AV was used as the reference to determine the secondary oxidation products. AVs were measured according to the European standard NF EN ISO 6885:2016.[19] The previously extracted oils of 2.5–5 mL were diluted in 25 mL of isooctane. This mixture (test solution) of 5 mL was transferred into a test tube, after which 1 mL of anisidine reagent was added. Additionally, an unreacted test solution, where acetic acid replaced the anisidine reagent, was prepared. A blank test was carried out with isooctane replacing the test solution. The test tubes were shaken and left in the dark. After 10 min of reaction, the absorbance of the solution was recorded at 350 nm. Pure isooctane was used as the blank for UV–Vis spectrophotometry (Shimadzu UV-1800) measurements. The AV is a dimensionless quantity. The experiments were done in quadruplicate.

2.4 | Total oxidation value

The oxidation state of the oil was expressed as the total oxidation value (TV), as determined by the following equation: $TV = 2 \times PV + AV$.[19]

Student's *t* tests were carried out at the $p < 0.05$ probability level using XLSTAT software (version 2022.3.2; Addinsoft, XLSTAT statistical and data analysis solution; https://www.xlstat.com 2023).

2.5 | Near infrared spectroscopy analysis

The emulsions were taken in round sealed glass bottles; all samples were homogenized for 30 s before analysis. NIR spectra were acquired using a Bruker MPA spectrometer (Bruker Optics) in reflectance mode (Figure 1). OPUS software version 7.2 (Bruker Optics) was used for instrument control and data acquisition. Each absorbance spectrum was collected by averaging 32 scans from 800 to 2779 nm with 0.86 nm resolution (2307 variables) with the light source illuminating the bottom of the bottle. Spectra were analyzed in triplicate; all the five samples were analyzed on 10 different days (J01–J04, J07–J11, and J15) for a total of 150 spectra ($3 \times 10 \times 5$).

2.6 | Preprocessing and statistical analysis of near-infrared spectral data

The 150 NIR spectra were processed while taking the Mahalanobis distance into consideration, with a threshold of 10% to eliminate spectra that significantly deviated from the central cluster; this helped to improve the quality and reliability of the obtained data. The first part of the statistical analysis was designed to target the characteristic wavelengths associated with aging (Figure 2). A first global Kruskal–Wallis test (5%) was used to study the differences between NIR absorbance at each wavelength (raw spectra), and aging (J01–J15) as a qualitative variable. A screening of the most significant spectral ranges *i*–*j* for aging was then carried out regarding the *p*-value, with a threshold of 5%. Days of aging were then divided into two groups: A and B (Group A includes days 1–7 [week 1], whereas group B comprises days 9–15 [week 2]), to perform a nonparametric Wilcoxon signed-rank test (5%) and compare the means of the two related groups. The absorbances corresponding to the n spectral columns contained between columns i and j of each *i*–*j* range were averaged to give one column per individual. This was repeated for all the significant spectral ranges found in the previous step. The second part of the statistical analysis was designed to predict the aging. The entire spectral data were then mathematically preprocessed to correct for light scattering effects, sharpen the peaks of interest, and remove multiplication noise and baseline variations. Seven types of preprocessing were tested: none (i.e., the raw data were used), first (D1), second (D2) and third (D3) derivative transformations of Savitzky–Golay, multiplicative scattering correction (MSC), standard normal variate (SNV), and SNV + Detrend.[20] Models for predicting peroxides, anisidine, and TVs were developed by using partial least squares discriminant analysis (PLS-DA) between the NIR spectra and the time periods A and B.[21] Both periods reflected the peroxide and *p*-AVs, and each model was challenged using cross-validation. Prediction accuracy and misclassification rates obtained from confusion matrices were calculated to assess the performance of each model. Four rates were calculated, namely, the true positive (TP) rate, the true negative (TN) rate, the false positive (FP) rate, and the false negative (FN) rate. TP is defined as the number of spectra from period B that were correctly classified, and TN is the share of

FIGURE 1 At-line analysis of emulsions by near infrared spectroscopy (NIRS) using Bruker MPA spectrometer.

spectra from period A that were correctly identified. As for FP, it specifies the proportion of spectra from period A wrongly classified as spectra from period B, whereas FN is the share of spectra from period B wrongly identified as spectra from period A. These rates can be used to calculate the classification error and prediction accuracy. Five indicators have been calculated to determine the performance of each model, namely, the precision, the predictive value of period A, the sensitivity, the specificity, and the accuracy. A high precision demonstrates the model's ability to accurately predict instances in period B while minimizing false predictions in this period. A high predictive value of period A indicates the model's effectiveness in accurately identifying instances that belong to period A. The sensitivity measures the model's capability to correctly identify the aged emulsions from period B. The specificity measures the model's ability to accurately identify the aged emulsion from period A, highlighting its capability to avoid false predictions in period B. The accuracy represents the overall effectiveness of the model in making correct predictions across both periods A and B and provides a holistic view of the model's performance. The five indicators are calculated from the following equations:

$$\text{Precision} = TP/(TP + FP)$$

$$\text{Predictive value of period A} = TN/(TN + FN)$$

$$\text{Sensitivity} = TP/(TP + FN)$$

$$\text{Specificity} = TN/(TN + FP)$$

$$\text{Accuracy} = (TP + TN)/(TP + FP + FN + TN)$$

The preprocessing of the spectral data, and the development of the models were done using MATLAB 9.4 with the SAISIR package, The Unscrambler (version X, CAMO Software AS), and XLSTAT software (version 2022.3.2; Addinsoft, XLSTAT statistical and data analysis solution; https://www.xlstat.com 2023).[22]

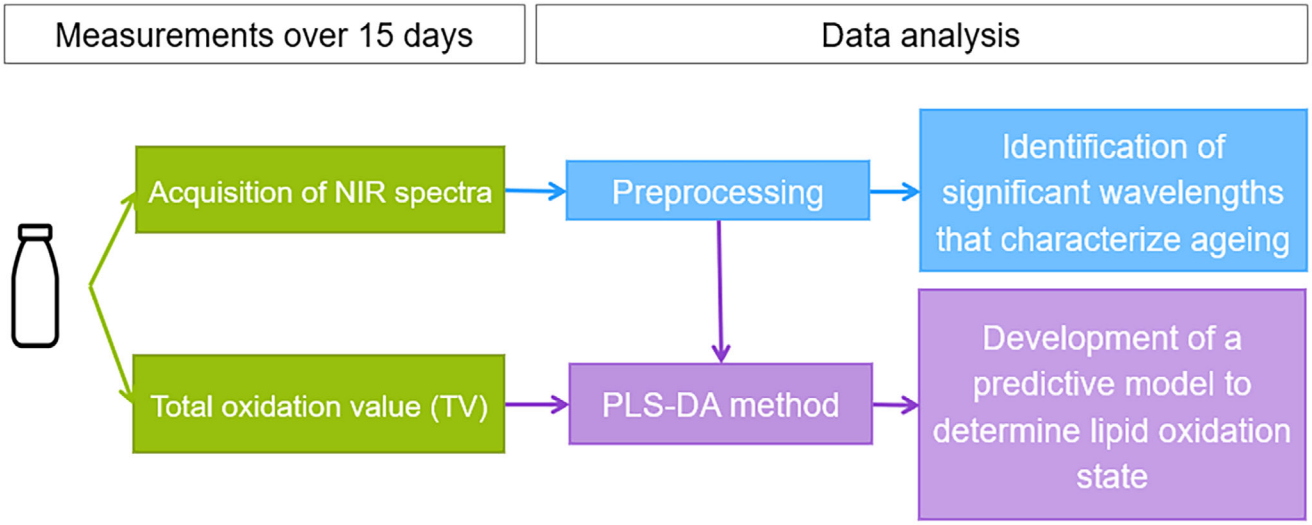

FIGURE 2 Methodology of data mining of the referenced near infrared (NIR) spectra.

3 | RESULTS AND DISCUSSION

3.1 | Titration values

The titration values listed in Table 1 show the evolution of the level of oxidation of the oil in the emulsion (Table 1). We observed that AVs increased during the oxidation step, which contributed to increasing the TV. Moreover, it is seen that PV reached a maximum around 4–8 days before showing a decrease beyond 9 days. The maximum of PV of the pre-polymerized oil is lower (close to 14 meq O_2 kg^{-1}) compared to a non-modified linseed oil.[23] In fact, the PV profile obtained is similar as the Gaussian curve of PV obtained for frying oils with maximum values around 14 meq O_2 kg^{-1}.[24] The Gaussian curve on Figure 3 seemed to correspond to the three phases of oxidation, namely, initiation, propagation, and termination, as described by Musakhanian et al.[7]

According to the AV in Table 1, the generation of aldehydes began almost simultaneously with the formation of hydroperoxides (initiation phase). The amount of aldehydes increased more rapidly in the middle of the steady state and continued to increase when the decomposition of hydroperoxides started. This observation was in accordance with the study of Guillén and Cabo on the oxidation of edible oils.[25]

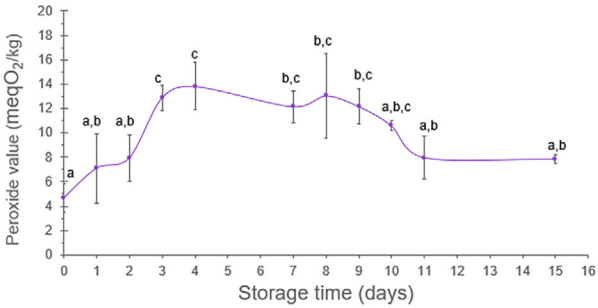

FIGURE 3 Changes in PV of the emulsion samples during 15-day storage at 50°C. The oxidative phases: ① Initiation and propagation phases; ② steady state; ③ termination phase. Different superscript letters imply that the values are statistically different ($p < 0.05$), using the Kruskal–Wallis test. The pairwise comparison was performed using the Conover-Iman test.

3.2 | Raw near infrared spectra

The 150 NIR spectra were processed considering Mahalanobis distance with a threshold of 10% to eliminate spectra that significantly deviated from the central cluster, helping to improve data quality

TABLE 1 Peroxide, anisidine, and total oxidation values of water-in-oil-in-water emulsion during the 15 days of aging.

	Time at 50°C (Day)										
	0	1	2	3	4	7	8	9	10	11	15
PV (meq O_2 kg^{-1})	4.7 ± 1.2^{a}	7.1 ± 2.9 a,b	7.9 ± 1.9 a,b	12.9 ± 1.0 c	13.8 ± 1.9 c	12.1 ± 1.3 b,c	13.0 ± 3.4 b,c	12.2 ± 1.5 b,c	10.6 ± 0.4 a,b,c	8.0 ± 1.8 a,b	7.8 ± 0.4 a,b
AV	3.4 ± 1.5^{a}	4.6 ± 1.5^{a}	5.7 ± 0.5 a,b	5.8 ± 1.0 a,b	7.7 ± 1.2 b,c	17.5 ± 2.1 d	13.8 ± 0.2 c	14.4 ± 0.5 c,d	19.1 ± 0.3 d,e	31.5 ± 5.7 e	28.3 ± 5.8 e
TV (meq O_2 kg^{-1})	12.7 ± 2.8	18.8 ± 5.9	21.5 ± 3.8	31.6 ± 2.2	35.3 ± 4.0	41.8 ± 3.3	39.8 ± 6.9	38.8 ± 3.0	40.3 ± 0.8	47.4 ± 6.7	44.0 ± 5.8

Note: Different superscript letters imply that the values are statistically different ($p < 0.05$), using the Kruskal–Wallis test. The pairwise was performed using the Conover-Iman test.

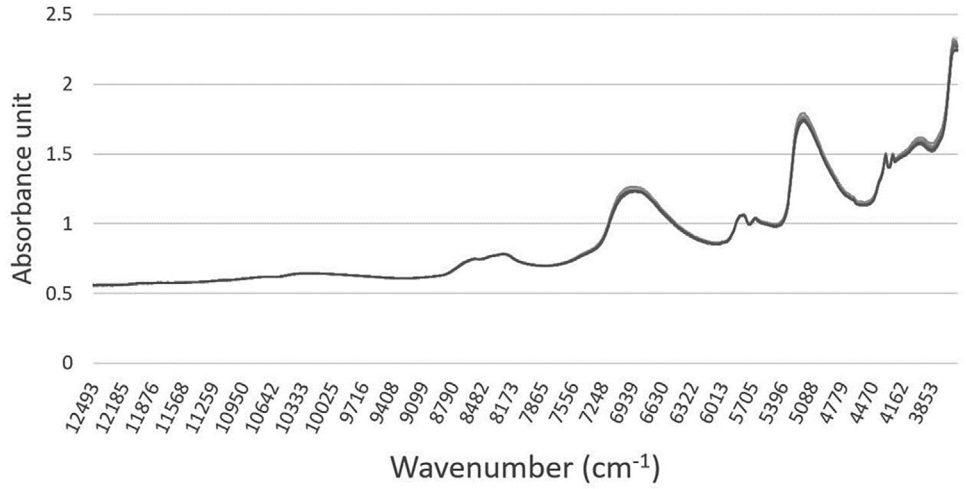

FIGURE 4 Overlay of 132 raw near infrared (NIR) spectra (3704–12 500 cm^{-1}) of oil (48% w/w) in water-in-oil-in-water (W/O/W) emulsion. Samples were stored in the dark at 50°C for 15 days.

and reliability. This processing resulted in 132 spectra for the 15 days of kinetic tracking. The 132 raw NIR spectra of the emulsion are represented in Figure 4. The collected spectra presented little noise.

3.3 | Link between wavelengths and aging period

A first global Kruskal–Wallis test (5%) was performed to study the differences between NIR absorbance at each wavelength (raw spectra) and the aging (J01–J15) as a qualitative variable. A screening of the most significant wavelengths was then carried out regarding the *p*-value, with a threshold of 5%. This resulted in the selection of three spectral ranges: 7541–5948, 5739–3657, and 3645–3637 cm^{-1} (equivalent to the wavelength ranges 1326–1681, 1742–2734, and 2743–2749 nm), which correspond to the first overtone and the combination band regions. According to Rodrigues et al., the 7541–5948 cm^{-1} region corresponds to –OH- and CH-stretching vibrations. In this work, it was also shown that the NIR spectral region from 10 000 to 6500 cm^{-1} is the range, including the bands of the functional groups involved in lipid oxidation.[26] The second region covering the 5739–3657 cm^{-1} range is related to CH-stretching vibrations of the cis double bound of unsaturated fatty acids. This region includes bands of C–H-stretching vibrations and the characteristic bands of the hydroperoxides (–OH combination bands and stretching vibrations), respectively, at 4800 and 6950 cm^{-1}.[26] The third region 3645–3637 cm^{-1} corresponds to hydroxyl groups, and the spectral region 3700–3100 cm^{-1} includes the stretching vibrations of hydroxyl from water, hydroperoxides, and breakdown compounds such as alcohols and aldehydes.[27]

We traced 132 spectra for 10 point modalities (J01–J04, J07–J11, and J15). The number of spectra per modality varied between 11 and 15 due to the cleaning performed with the Mahalanobis distance. As the number of individuals per modality must be the same to perform the nonparametric Wilcoxon signed-rank test, only the first 11 spectra of each "day" modality have been kept, for a total of 110 spectra (11 spectra × 10 days). Figure 5 shows a visual summary of the Wilcoxon test results in the form of box-plot graphs. For the three spectral ranges, the *p*-value is clearly below 5%, meaning that periods A and B are significantly different. We can see that for these spectral ranges, the absorbance of the bands decreases from periods A to B. This observation could be explained by a loss in *cis* double bonds and hydroperoxides during lipid oxidation. According to Fang et al., the decrease of the OH-stretching band around 3640 cm^{-1} can be attributed to the decomposition of hydroperoxides.[28] The decrease in hydroperoxides was also observed when using the titration method (Figure 3). Indeed, the decomposition of hydroperoxides takes place during the termination phase at 9 days, which is in agreement with the lower absorbance of period B as compared to period A (Figure 5).

TABLE 2 Averaged index values for periods A and B.

	Averaged PV (meq O_2 kg^{-1})	Averaged AV	Averaged TV (meq O_2 kg^{-1})
Period A	10.77	8.25	29.79
Period B	10.32	21.43	42.08
p-Value of Student's *t*-test	0.858	0.009	0.02

The results showed that it is possible to highlight spectral differences between moderate oxidation levels (period A) and increased oxidation levels (period B). The selected mathematical models have been successful in predicting if an emulsion belongs to period A or B according to its IR spectrum. Moreover, a *t*-test showed that the averaged aging values for anisidine and the total oxidation are statistically significant (*p*-value <0.05) (Table 2). Therefore, considering the TV, it seems to be an appropriate reference method for the NIRS model.

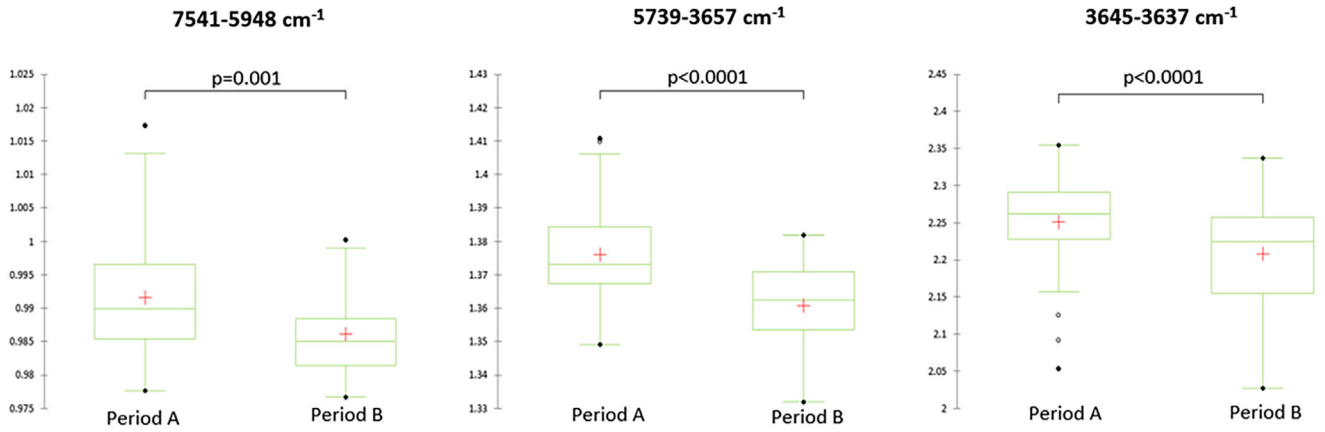

FIGURE 5 Box-plot graphs of the nonparametric Wilcoxon test results.

TABLE 3 Performances of prediction models based on the 132 raw and pre-processed near infrared (NIR) spectra to predict the aging of the emulsions.

Preprocessing	TN	TP	FN	FP	Precision (%)	Predictive value of Period A (%)	Sensitivity (%)	Specificity (%)	Accuracy (%)
Raw	52	67	1	12	85	98	99	81	90
MSC	52	67	1	12	85	98	99	81	90
SNV	51	68	0	13	84	100	100	80	90
SNV + Detrend	48	65	3	16	80	94	96	75	86
Derivative 1	18	32	36	46	41	33	47	28	38
Derivative 2	14	31	37	50	38	27	46	22	34
Derivative 3	17	25	43	47	35	28	37	27	32

Abbreviations: FN, false negative rate; FP, false positive rate; MSC, multiplicative scattering correction; SNV, standard normal variate; TN, true negative rate; TP, true positive rate.

3.4 | Developing a model to predict the oxidation state of lipids

PLS-DA models have been developed on raw and pre-treated NIR spectra. Five indicators have been used to describe the performances of the seven models (Table 3). Results in Table 3 show that the raw, MSC, SNV, and SNV + Detrend preprocessed spectra lead to proper predictions for the aging process as compared to the three derivative transformation models. The preprocessing MSC and SNV are generally used to enhance the quality of spectra by eliminating or reducing undesirable effects such as light scattering. The similarity of the MSC model and the raw spectra seems to indicate that measuring through the glass container did not have any influence on the spectral data. This similitude suggests that the quality of the raw spectra is satisfactory, and given the current sample size, a correction related to light scattering is not needed. The high precision of the MSC model demonstrates its ability to accurately predict the spectra from period B while minimizing false predictions. The predictive value of period A seems higher for the SNV model. Concerning sensitivity, the SNV model is the best, followed by the MSC, which in turn, is better than the ones with no pretreatment. The specificity is higher for the raw spectra and for the MSC model. A better accuracy of the tested preprocessing steps is obtained with the raw, MSC- and SNV-pretreated NIR spectra.

The method to design the predictive model based on the acquisition of NIR spectra of emulsions through glass bottles saved a considerable amount of time by allowing a direct analysis without sampling. It was thought that this operation may lead to variability because of differences with respect to the container. In fact, the PLS-DA showed good performances with both the raw and MSC preprocessed spectra. This absence of interference conferred good reliability to the method: A predictive model can be successfully applied to determine the lipid oxidation state of an emulsion by NIR stored in a glass-sealed container. Thus, this method could be applied to *at-line* or *off-line* monitoring for quality control of formulations in industry. To the best of our knowledge, there have been no reports on the assessment of lipid oxidation in emulsions using noninvasive methods such as NIRS. Existing studies have generally focused on NIR spectroscopy using a fiber optic probe.[9,26] The predictive model developed within this research has exhibited good performance considering that a noninvasive method was used to monitor the oxidation process.

The model's performances were evaluated through cross-validation. This method involves dividing the dataset into several subsets, then training the model on one subset and testing it on the rest of the data. This process is repeated multiple times with different data partitions. On the other hand, external validation involves splitting the dataset into two distinct sets: a training set used to train the model and a test set used to evaluate its performance. The test data are not used during model training. In our study, cross-validation was preferred due to the limited size of the dataset. In cross-validation, all spectra are used for both training and validation, but at different times, following a specific partitioning scheme. Conversely, in external validation, the test data are excluded from model training and only used to evaluate performance after training. The choice of validation method is crucial for estimating model robustness and generalization ability. Therefore, cross-validation results are typically used to adjust model parameters and assess its ability to generalize to new data, whereas external validation results are used to estimate the model's actual performance on unknown data, providing insights into its stability under different experimental conditions, for example.

In fact, to improve the model's performance, it would be useful to increase the number of samples. Sample numbers could be increased by doing measurements in triplicate and/or by increasing the number of days of aging. It would also be interesting to include samples aged under ambient temperature conditions into the predictive model for a more comprehensive analysis.

Expanding the dataset to include a greater diversity of samples would likely overcome the limitations of this study. Another avenue for improvement would be the use of a different validation method, such as validation on an independent dataset, thereby validating the model's ability to generalize to other datasets.

4 | CONCLUSIONS

The quality of emulsions can be compromised by lipid oxidation, a complex process, difficult to predict. We have studied the process of lipid oxidation in a typical emulsion that has applications in cosmetics, pharmaceutics, food, or coatings industry. Lipid oxidation was induced under accelerated aging conditions at 50°C for 15 days, and NIR spectra were recorded in situ through the glass sample containers. Three spectral ranges were identified that best discriminate spectral data analysis, namely, 7541–5948, 5739–3657, and 3645–3637 cm^{-1}. Therefore, we have shown that NIRS is adapted as a versatile tool to monitor lipid oxidation in a water-in-oil-in-water emulsion (48% w/w of oil).

Indeed, NIRS coupled with PLS-DA allowed to correctly classify the emulsions as a function of the oxidation duration. The best performances were obtained with raw and MSC preprocessed spectra corresponding to a precision of 85%, a predictive value of 98% for period A, a sensitivity of 99%, a specificity of 81%, and an accuracy of 90%. These results also suggest that correction related to light scattering was not required for this sample size. Thus, NIRS stands out as a unique measurement technique that is both nondestructive and environmentally friendly, avoiding extraction steps that use hazardous solvents. Noninvasive measurements offer a valuable option in the analysis of samples stored in bottles as part of a quality control protocol. This approach thus enables sample examination without opening the packaging, thereby maintaining the marketability of products.

AUTHOR CONTRIBUTIONS

Conceptualization; formal analysis; investigation; writing—original draft; visualization: Laetitia Boisset. Conceptualization; resources; writing—original draft; visualization: Pascale de Caro. Investigation; validation: Ivana Stojmilovic. Project administration; conceptualization; funding acquisition; writing—review and editing: Sophie Thiebaud-Roux. Conceptualization; methodology; formal analysis; resources; data curation; writing—original draft; writing—review and editing: Cécile Levasseur-Garcia.

ACKNOWLEDGMENTS

The authors thank the National agency for research and technology (ANRT) for financial support. Financial and technical support from Colibri is acknowledged. This work was also supported by the French state through the National Research Agency under the Program for Future Investments bearing the reference ANR-18-EURE-0021.

CONFLICT OF INTEREST STATEMENT

The authors have declared no conflicts of interest.

DATA AVAILABILITY STATEMENT

The data that support the findings of this study are available from the corresponding author upon reasonable request.

REFERENCES

1. Tadros, T. F. (2016). *Emulsions: formation, stability, industrial applications*. De Gruyter.
2. Zhang, N., Li, Y., Wen, S., Sun, Y., Chen, J., Gao, Y., Sagymbek, A., & Yu, X. (2021). Analytical methods for determining the peroxide value of edible oils: A mini-review. *Food Chemistry*, *358*, 129834.
3. Berton-Carabin, C. C., Ropers, M.-H., & Genot, C. (2014). Lipid oxidation in oil-in-water emulsions: Involvement of the interfacial layer. *Comprehensive Reviews in Food Science and Food Safety*, *13*(5), 945–977.
4. Keramat, M., Kheynoor, N., & Golmakani, M.-T. (2022). Oxidative stability of Pickering emulsions. *Food Chemistry: X*, *14*, 100279.
5. Poyato, C., Navarro-Blasco, I., Calvo, M. I., Cavero, R. Y., Astiasarán, I., & Ansorena, D. (2013). Oxidative stability of O/W and W/O/W emulsions: Effect of lipid composition and antioxidant polarity. *Food Research International*, *51*(1), 132–140.
6. Alam, M., Akram, D., Sharmin, E., Zafar, F., & Ahmad, S. (2014). Vegetable oil based eco-friendly coating materials: A review article. *Arabian Journal of Chemistry*, *7*(4), 469–479.
7. Musakhanian, J., Rodier, J.-D., & Dave, M. (2022). Oxidative stability in lipid formulations: A review of the mechanisms, drivers, and inhibitors of oxidation. *AAPS PharmSciTech*, *23*(5), 151.
8. ten Klooster, S., Boerkamp, V., Lazaridi, E., Yang, S., Takeuchi, M., Berton-Carabin, C., Schroën, K., Janssen, H.-G., Friedrich, H., Hohlbein, J., van Duynhoven, J., & Hennebelle, M. (2022). Lipid oxidation in food emulsions: Analytical challenges and recent developments. In C. Bravo-Diaz (Ed.), *Lipid oxidation in food and biological systems* (pp. 3–29). Springer International Publishing.

9. Daoud, S., Waschatko, G., Bou-Maroun, E., & Cayot, P. (2020). Fast, direct and in situ monitoring of lipid oxidation in an oil-in-water emulsion by near infrared spectroscopy. *Analytical Methods*, *12*(24), 3098–3105.
10. Coupland, J. N., & McClements, D. J. (1996). Lipid oxidation in food emulsions. *Trends in Food Science & Technology*, *7*(3), 83–91.
11. Liu, J., Wang, Y. J., Huang, X. Y., Li, X. Z., Ma, C. G., & McClements, D. J. (2022). NMR analysis of lipid oxidation in flaxseed oil-in-water emulsions. *Journal of Agricultural and Food Chemistry*, *70*(27), 8417–8429.
12. Daoud, S., Bou-maroun, E., Dujourdy, L., Waschatko, G., Billecke, N., & Cayot, P. (2019). Fast and direct analysis of oxidation levels of oil-in-water emulsions using ATR-FTIR. *Food Chemistry*, *293*, 307–314.
13. Hayati, I. N., Man, Y. B. C., Tan, C. P., & Aini, I. N. (2005). Monitoring peroxide value in oxidized emulsions by Fourier transform infrared spectroscopy. *European Journal of Lipid Science and Technology*, *107*(12), 886–895.
14. Vinet, J., Tréguier, S., Levasseur-Garcia, C., Calmon, A., & Violleau, F. (2022). Iodine and peroxide index rapid determination by mid- and near-infrared spectroscopy in ozonated sunflower oil and ozonated fats. *Ozone: Science & Engineering*, *44*(4), 337–350.
15. Richard, R., Li, Y., Dubreuil, B., Thiebaud-Roux, S., & Prat, L. (2011). On-line monitoring of the transesterification reaction between triglycerides and ethanol using near infrared spectroscopy combined with gas chromatography. *Bioresource Technology*, *102*(12), 6702–6709.
16. Armenta, S., Moros, J., Garrigues, S., & de la Guardia Cirugeda, M. (2010). Chapter 58: Determination of olive oil parameters by near infrared spectrometry. In *Olives and olive oil in health and disease prevention* (pp. 533–544). Elsevier/Academic Press.
17. Godfroid, T., Poussard, L., Poelman, M., Peeterbroeck, S., Danneaux, F., Holvoet, J.-P., & Michiels. (2020). *Device for electrically processing a fatty substance of plant origin* (WO 2018/002329). WIPO.
18. AFNOR NF EN ISO 27107. (2010). *Animal and vegetable fats and oils – Determination of peroxide value – Potentiometric end-point determination.*
19. AFNOR NF EN ISO 6885. (2016). *Animal and vegetable fats and oils – Determination of anisidine value.*
20. Agelet, L. E., & Hurburgh, C. R. (2010). A tutorial on near infrared spectroscopy and its calibration. *Critical Reviews in Analytical Chemistry*, *40*(4), 246–260.
21. Martens, H., & Naes, T. (1989). *Multivariate calibration*. J. Wiley & sons.
22. Cordella, C. B. Y., & Bertrand, D. (2014). SAISIR: A new general chemometric toolbox. *TrAC Trends in Analytical Chemistry*, *54*, 75–82.
23. Douny, C., Razanakolona, R., Ribonnet, L., Milet, J., Baeten, V., Rogez, H., Scippo, M.-L., & Larondelle, Y. (2016). Linseed oil presents different patterns of oxidation in real-time and accelerated aging assays. *Food Chemistry*, *208*, 111–115.
24. Karakaya, S., & Şimşek, Ş. (2011). Changes in total polar compounds, peroxide value, total phenols and antioxidant activity of various oils used in deep fat frying. *Journal of the American Oil Chemists' Society*, *88*(9), 1361–1366.
25. Guillén, M. D., & Cabo, N. (2002). Fourier transform infrared spectra data versus peroxide and anisidine values to determine oxidative stability of edible oils. *Food Chemistry*, *77*(4), 503–510.
26. Rodrigues, B. V. C., Pompeu, D. R., & Herman, C. A. N. P. (2021). Evaluation of quality parameters of açaí oil during thermal oxidation using NIRS and chemometrics. *Food Analytical Methods*, *14*(11), 2335–2345.
27. Belhaj, N., Arab-Tehrany, E., & Linder, M. (2010). Oxidative kinetics of salmon oil in bulk and in nanoemulsion stabilized by marine lecithin. *Process Biochemistry*, *45*(2), 187–195.
28. Fang, H. L., & McCormick, R. L. (2006). *Spectroscopic Study of Biodiesel Degradation Pathways* (SAE Technical Paper 2006-01–3300).

How to cite this article: Boisset, L., de Caro, P., Stojmilovic, I., Thiebaud-Roux, S., & Levasseur-Garcia, C. (2024). Monitoring lipid oxidation in multiple emulsions by near infrared spectroscopy. *European Journal of Lipid Science & Technology*, *126*, e2300267. https://doi.org/10.1002/ejlt.202300267